Design of a 200 MeV LINAC

ADS Roadmap

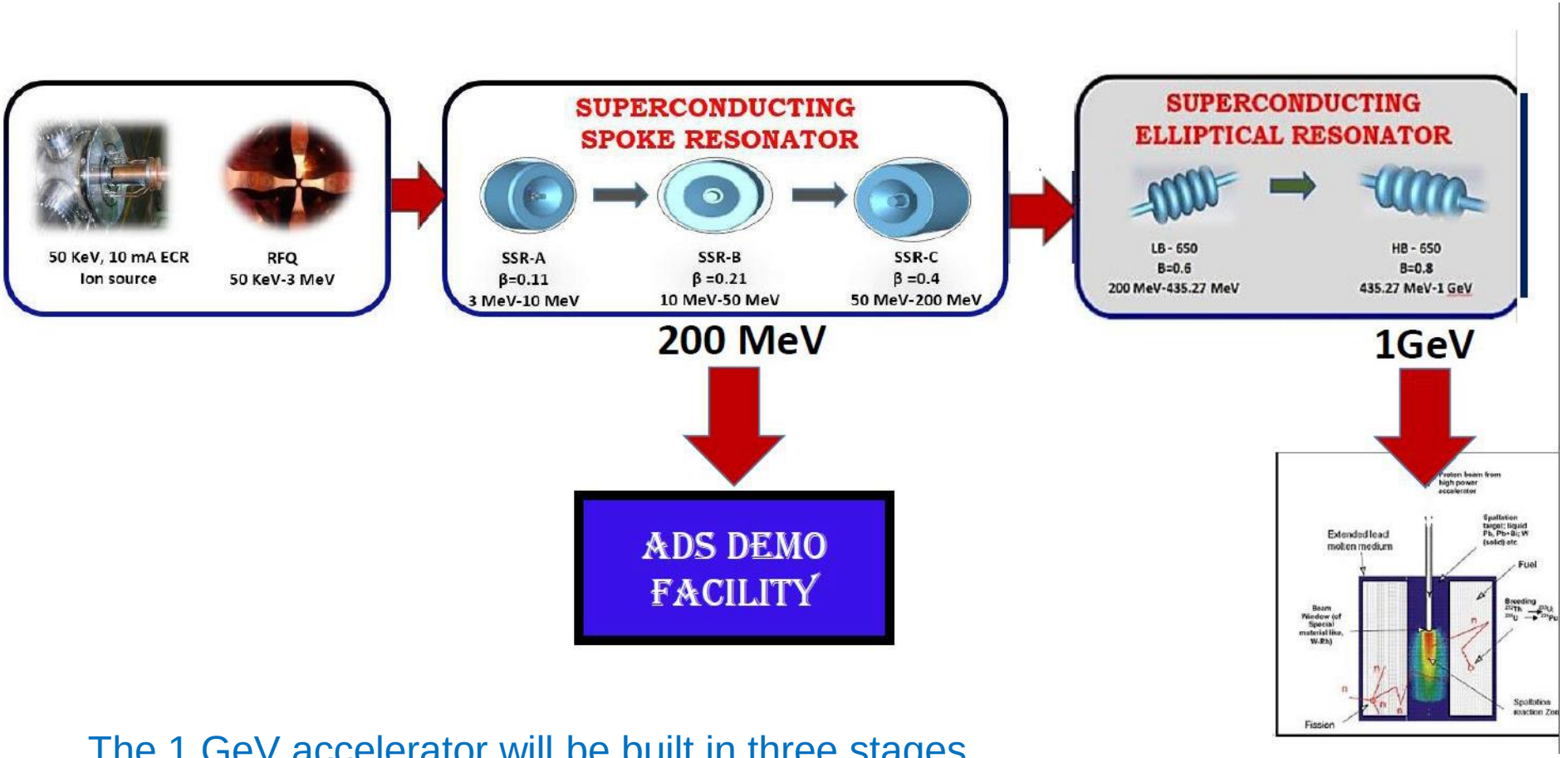

The 1 GeV accelerator will be built in three stages.

- Stage 1: 20 MeV LEHIPA being built at BARC
- Stage 2: 200 MeV Linac
- Stage 3: 1 GeV Linac

Most cost effective way to produce neutrons

- By Spallation process with GeV energy protons striking on high Z target.
- Number of neutrons per proton per Watt of beam power reaches a plateau just above 1 GeV.

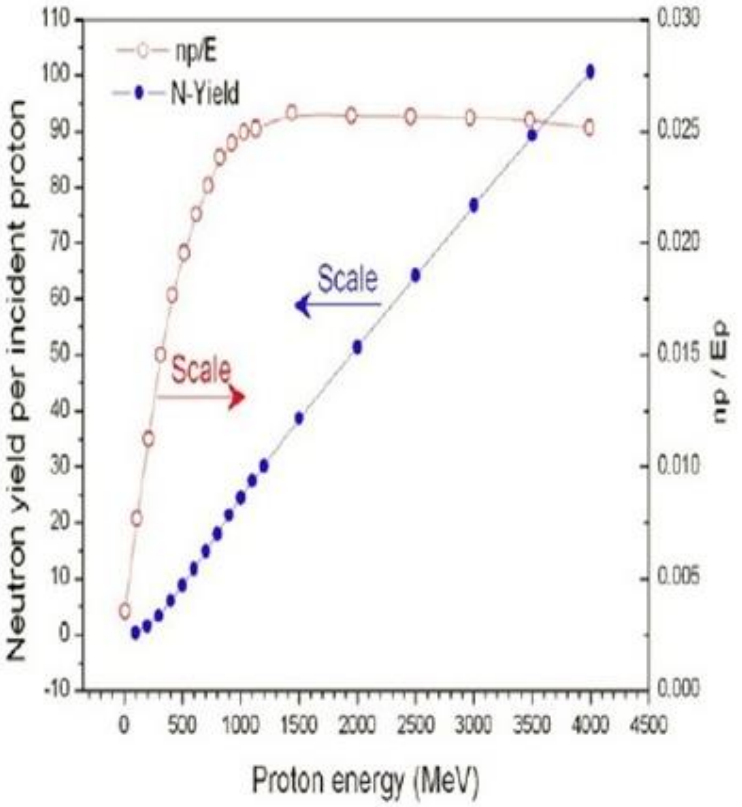

Neutrons production from spallation

Requirements from the accelerator for ADS

The accelerator is required to deliver 10's of mA of proton beam current in CW mode.

- High Reliability
- High Beam Power
- CW Operating Mode
- High Conversion Efficiency
- Minimum Beam Loss
- Easy Maintenance & Serviceability

The technologically most important and challenging part in ADS scheme is the High Power Proton Accelerator.

Accelerator for ADS

- **The Linac is divided into three parts for convenience.**
  - **Low Energy (upto 20 MeV)**
  - **Medium Energy (20 MeV to 200 MeV)**
  - **High Energy (200 MeV-1GeV)**

- **The accelerating structures used at different energies are:**
  - **Low Energy – RFQ**
  - **Medium Energy – DTL, CCDTL, SSR**
  - **High Energy – Elliptical Cavities**

- **Design issues are:**
  - **Beam loss control (< 1 W/m).**
  - **Formation of beam Halos.**
  - **Emittance growth.**
  - **Thermal Management.**

200 MeV LINAC Organization (MEHIPA)

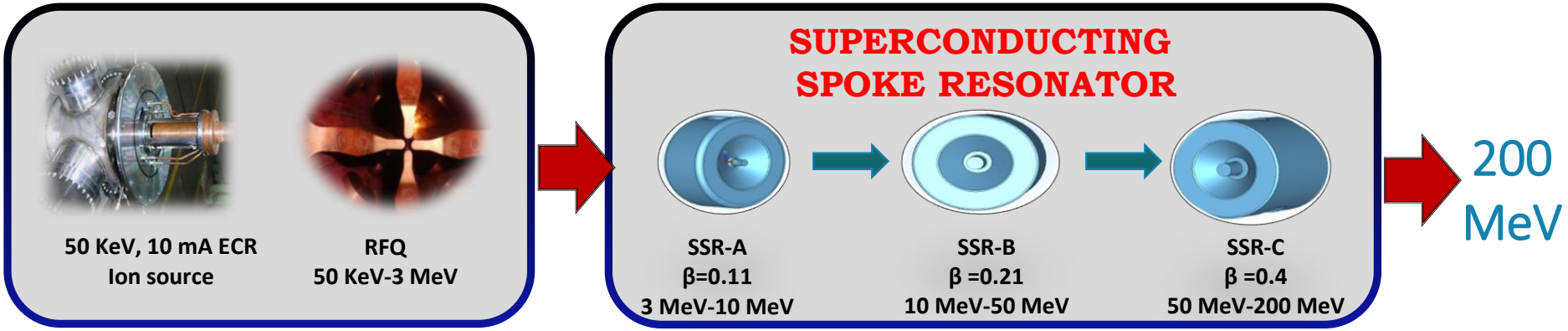

Accelerating structure	Energy Range
RFQ	50 keV - 3 MeV
SSR-A	3 - 10 MeV
SSR-B	10 - 50 MeV
SSR-C	50 - 200 MeV

Low Energy Beam Transport Line

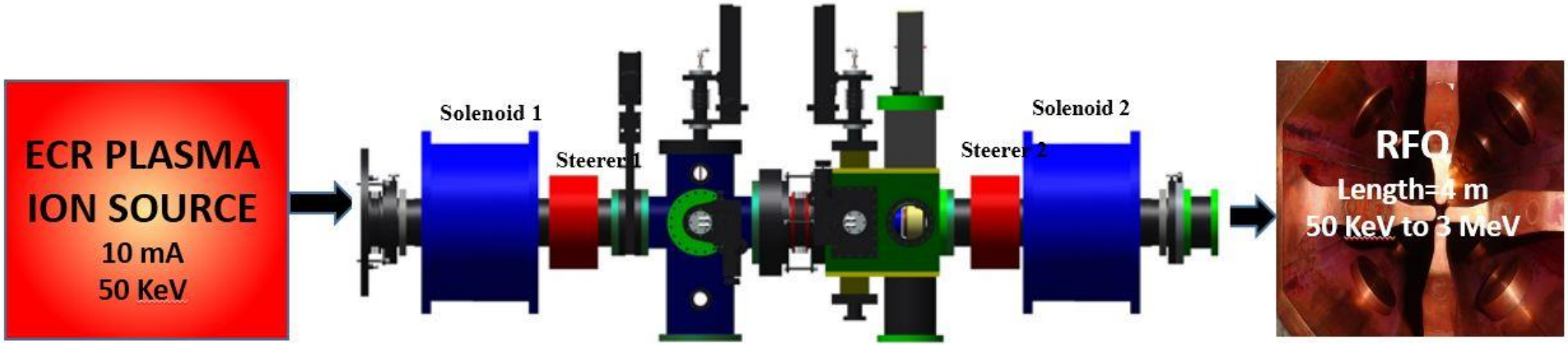

- Transport & Match the beam from ion source to the RFQ with minimum emittance growth.
- Reject the unwanted species from the ion source from entering the RFQ.
- Includes useful diagnostics for monitoring the beam from ion source.
- Matching is done using 2 solenoids.

LEBT: Focusing scheme

Parameter	Value
Input Emittance	0.2 π mm mrad
Beam Current	10 mA
Input Energy	50 keV
SCC	95 %

Two solutions are possible for matching the beam in the LEBT to the RFQ input.

- **Scheme-1: Weak Focusing**

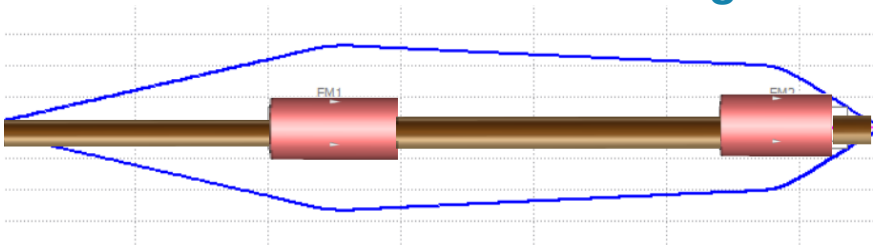

- **Scheme-2: Strong Focusing**

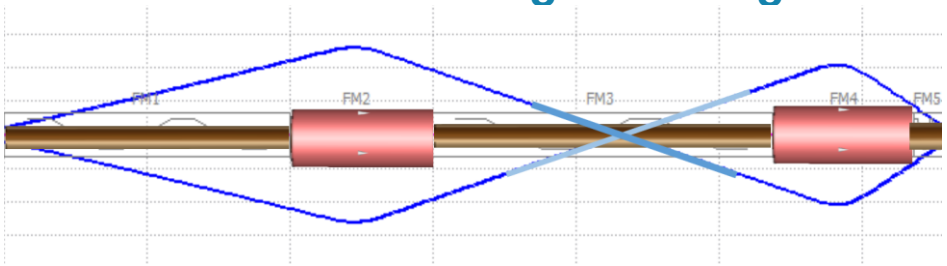

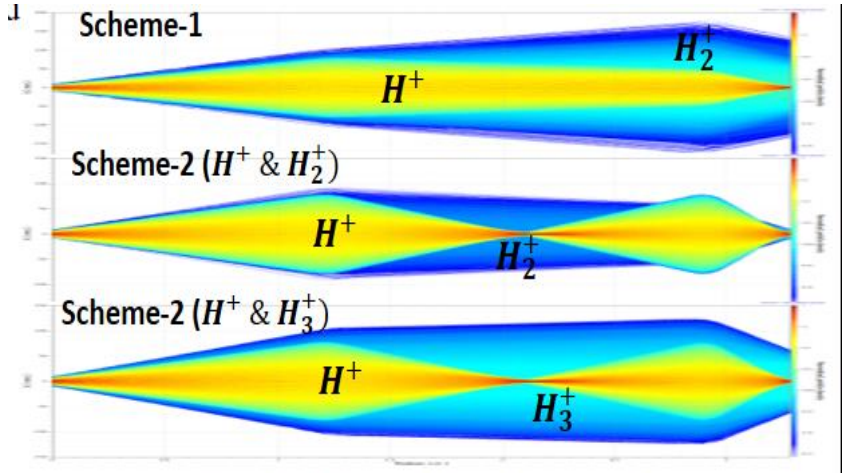

Fig ; Density plots for both focusing schemes.

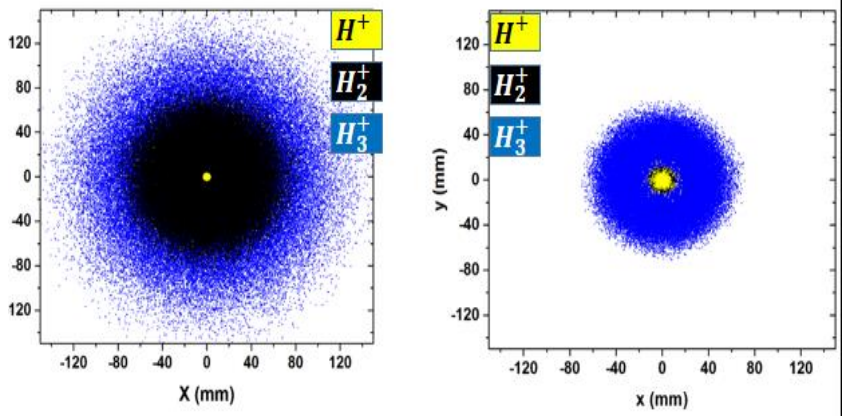

Fig ; Transverse distribution, (a)Scheme-1, (b) Scheme-2..

Scheme 1 is used as it shows lower emittance growth and better elimination of unwanted species in the LEBT by putting a slit at the end.

LEBT: Space Charge Compensation Studies

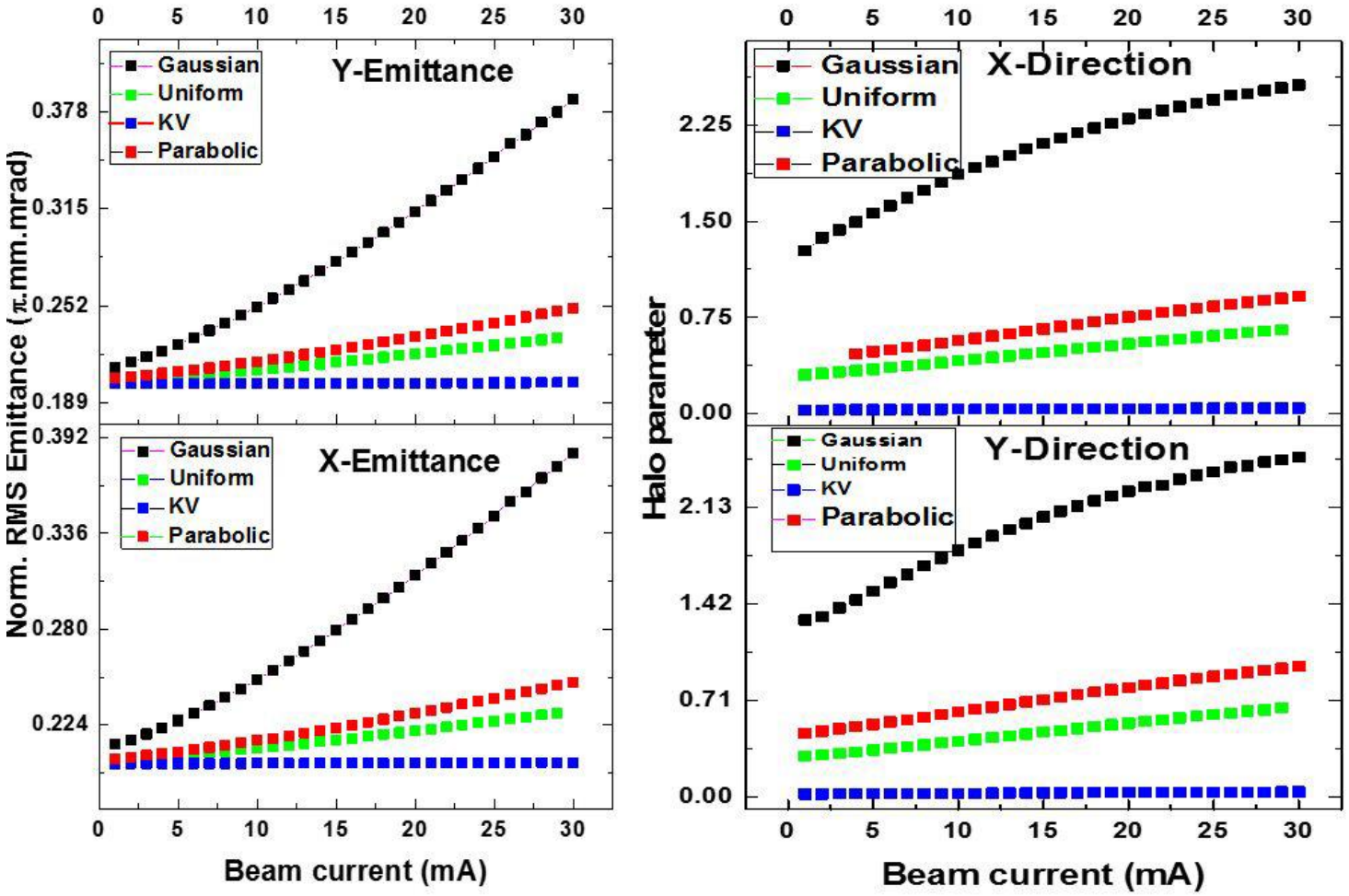

As the degree of space charge compensation increases the effective beam current decreases. Beam emittance and Halo formation decrease with increasing space charge compensation.

LEBT Beam Dynamics

- **LEBT simulations were performed with a 50 keV, 10 mA Gaussian beam with a space charge compensation of 95 %.**
- **To obtain the RFQ acceptance beam ellipse, solenoid S1 and S2 were tuned such that waist formation between them can be avoided that can lead to an emittance blow-up.**
- **Even with 95 % SCC, beam suffers an emittance blow-up of 12.5 % leading to a final value of 0.22 $\pi . mm - mrad$**

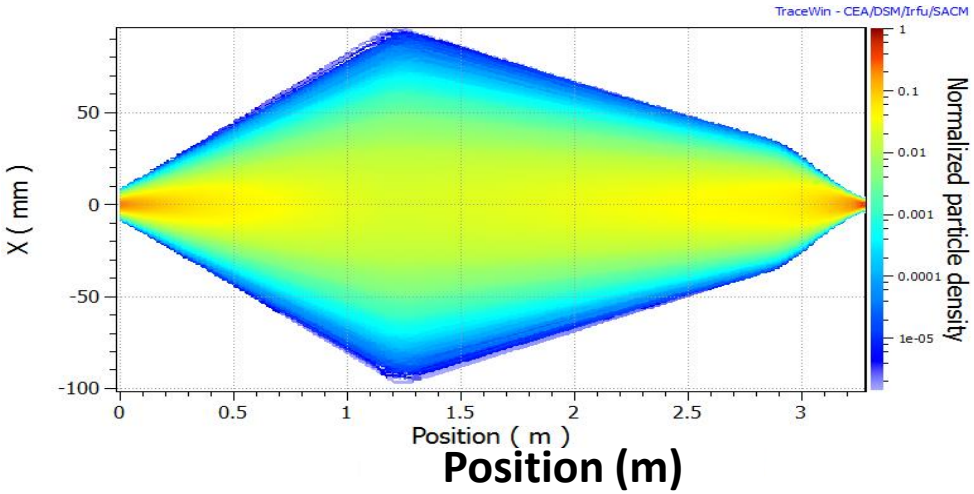

Transverse particle density distribution along the LEBT

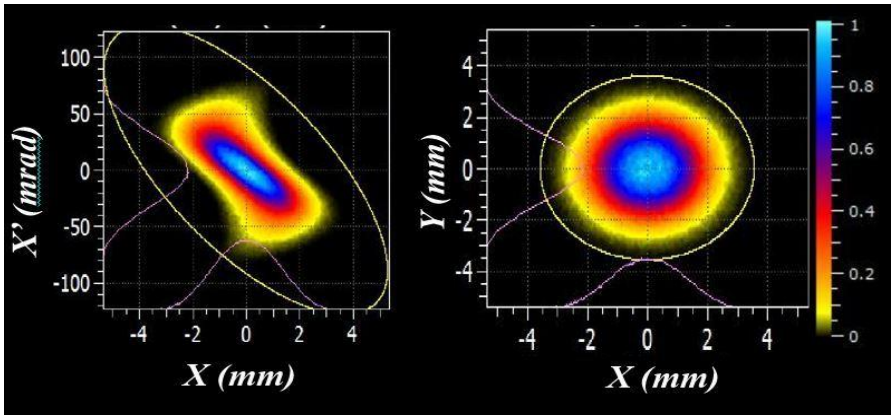

LEBT output distribution

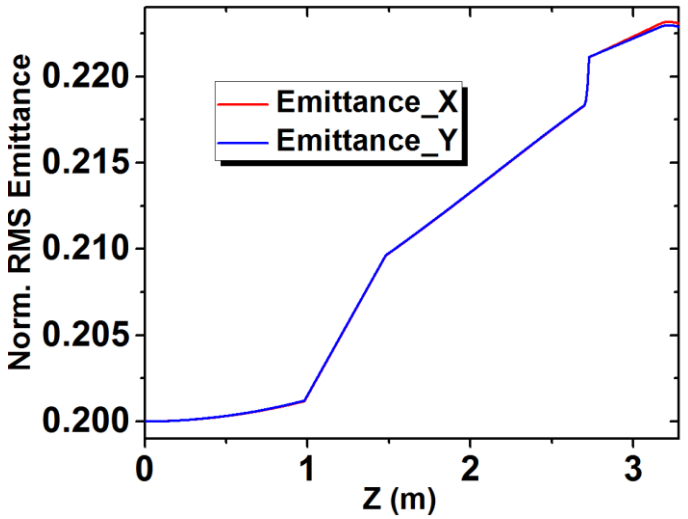

Norm. RMS emittance growth along LEBT

RFQ

Role of beam current in RFQ design

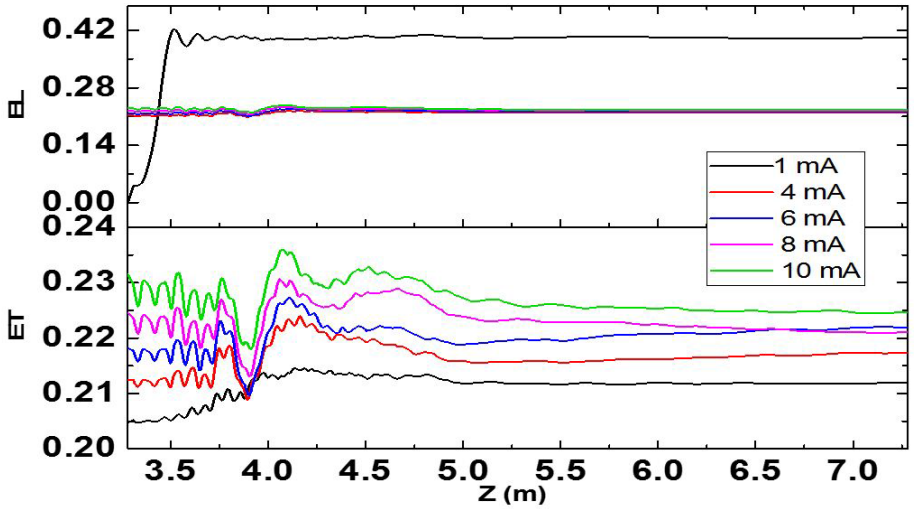

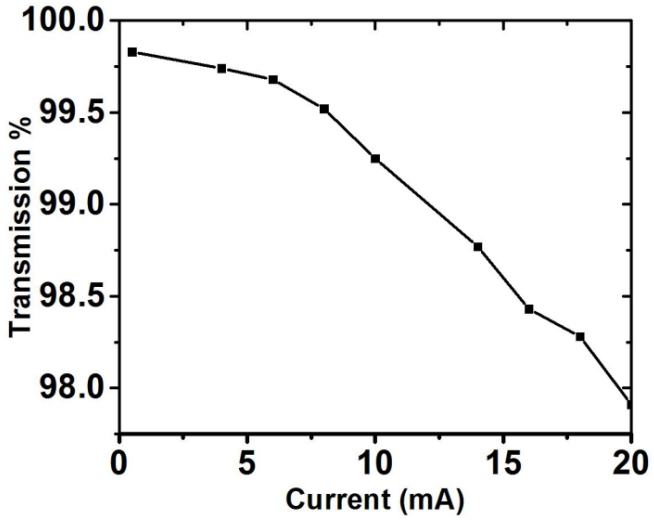

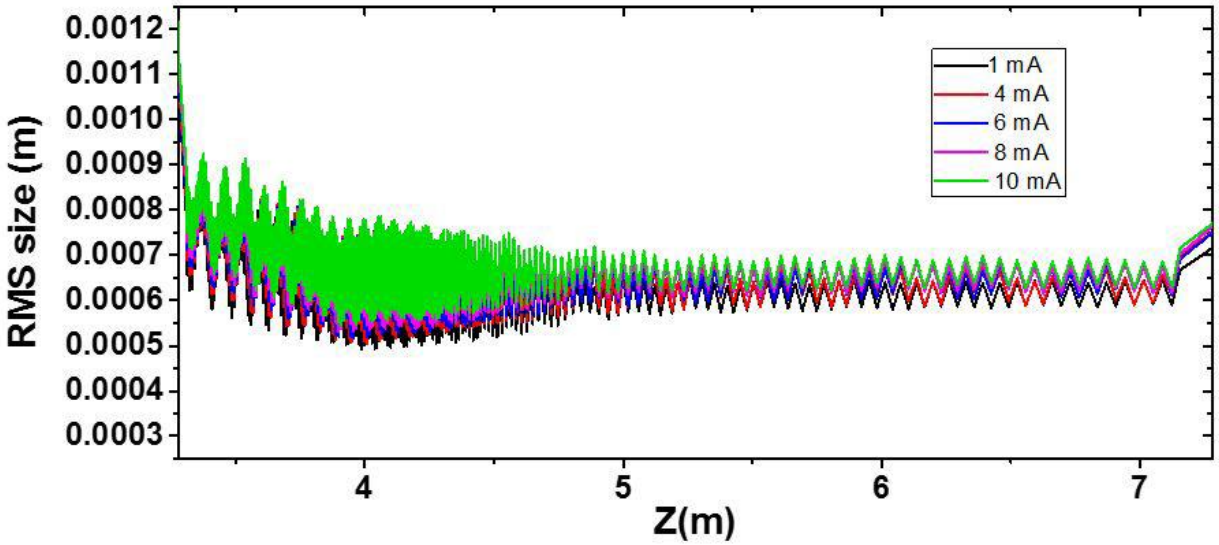

The final RFQ design has been done for a beam current of 10 mA.

RFQ Design

- **The beam from the LEBT is further propagated through a 4.02 m, 3 MeV RFQ with a full current of 10 mA, in the absence of SCC.**

Parameter	Value
Input energy (MeV)	0.05
Output energy (MeV)	3
Duty factor (%)	100
Frequency (MHz)	325
Beam current (mA)	10
RF Power (kW)	400
Transmission	99.03%
Output ε_x (π mm mrad)	0.221
Output ε_y (π mm mrad)	0.223
Output ε_z (π mm mrad)	0.2275
Vane voltage (kV)	80
Synchronous phase	-30
Length (m)	4

RFQ Beam Dynamics

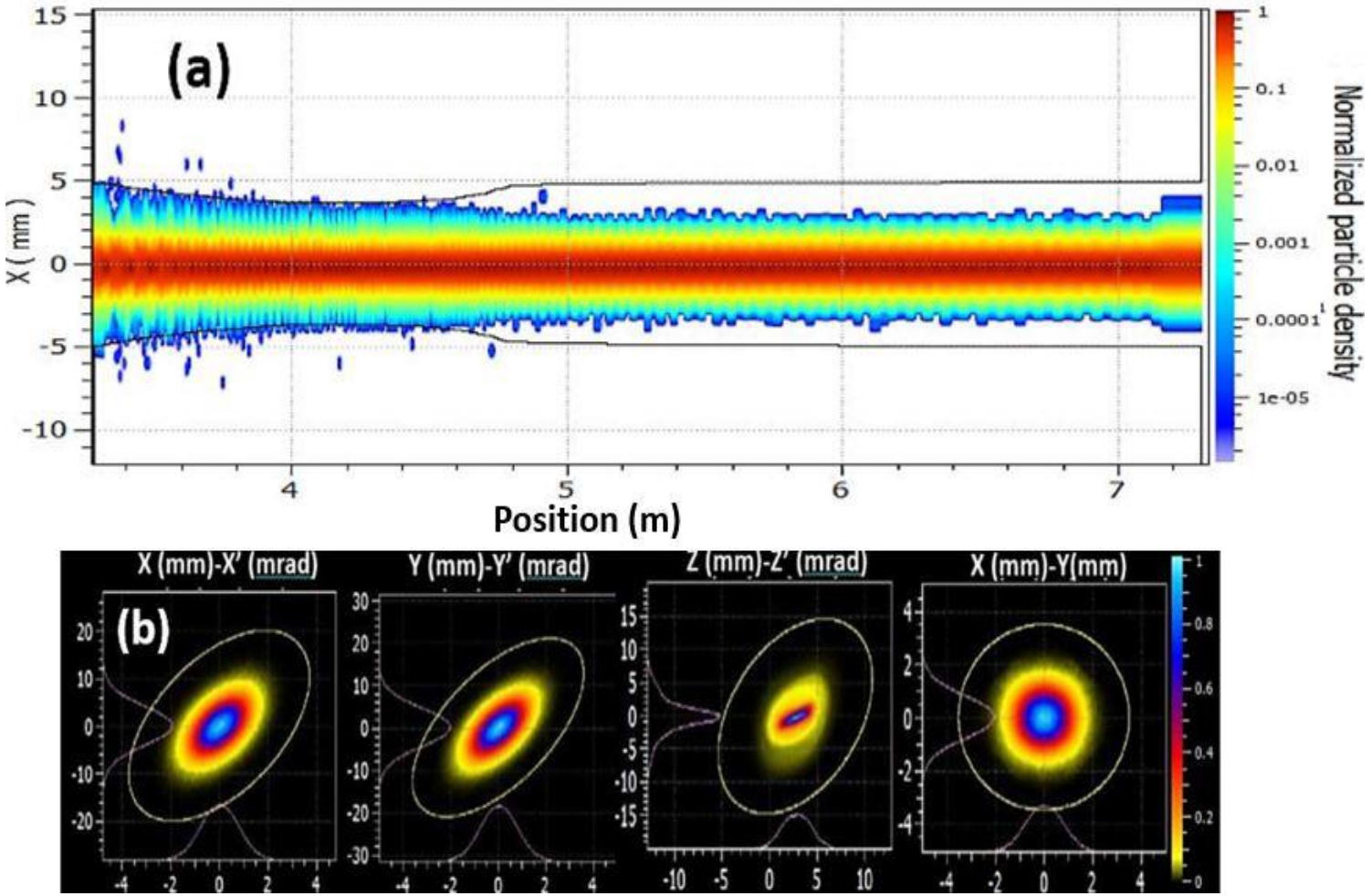

(a) Beam envelope along the RFQ, (b) phase space (x-x', y-y' and z-z') and coordinate (x-y) space particle distribution at the exit of RFQ, for a current of 10 mA.

RFQ Beam Dynamics

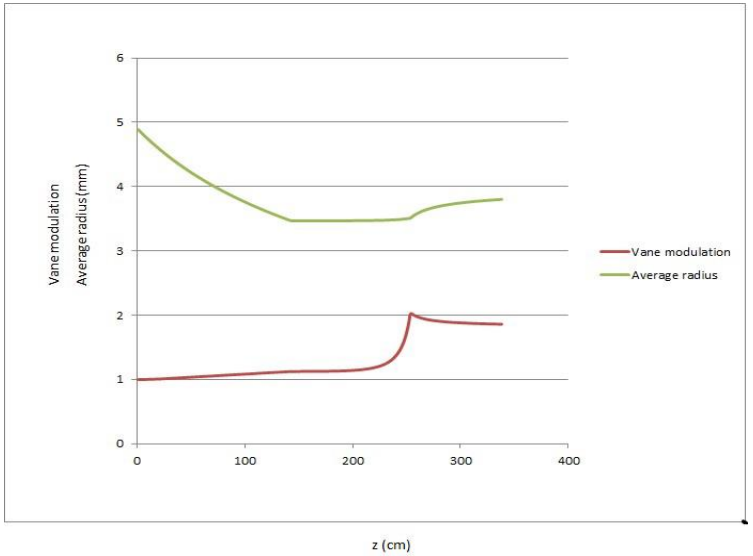

Variation of the modulation and average radius along the RFQ.

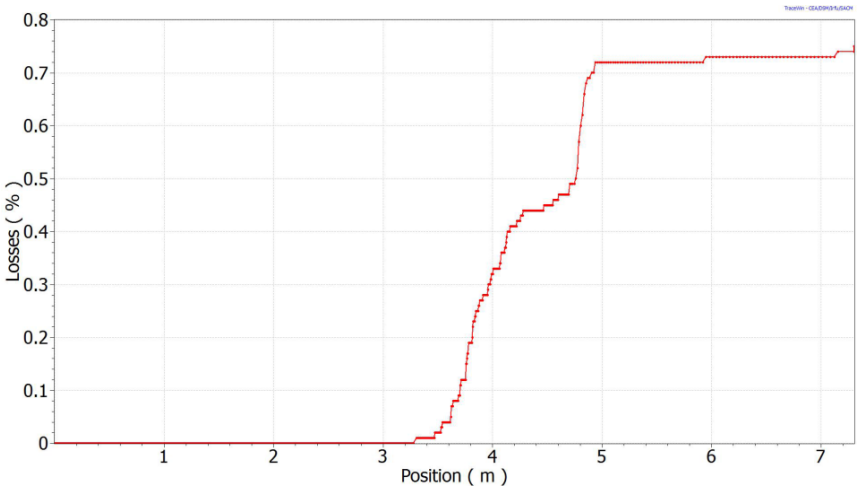

Percentage beam loss along the RFQ.

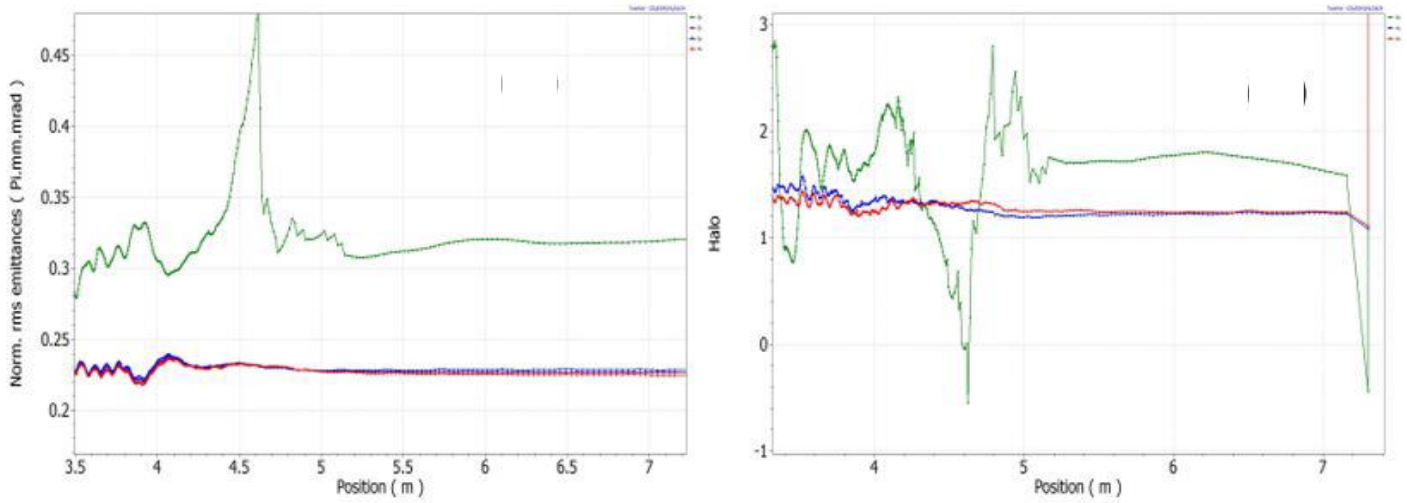

(a) Normalised RMS emittance and (b) halo parameter, through the RFQ.

MEBT

- Output beam from RFQ is matched to the spoke resonators through a medium energy beam transport (MEBT) line.
- The MEBT consists of 4 quadrupoles and two buncher cavities.

Parameter	Value
Total length (m)	0.97
Quadrupole1 gradient (T/m)	19.69
Quadrupole2 gradient (T/m)	39.53
Quadrupole3 gradient (T/m)	37.02
Quadrupole4 gradient (T/m)	36.31
RF Gap1 E0TL (kV)	67.75
RF Gap E0TL (kV)	71.01

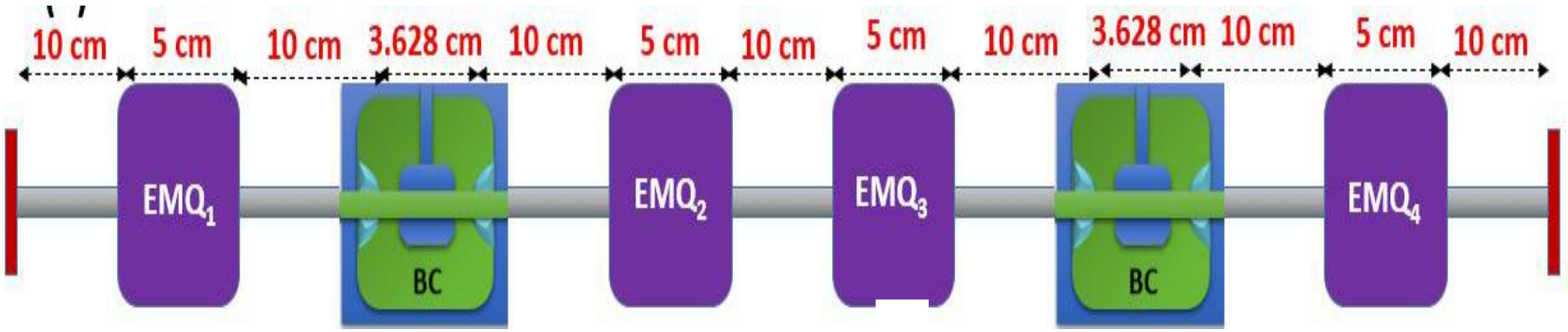

MEBT Simulation Results

Beam envelope along MEBT

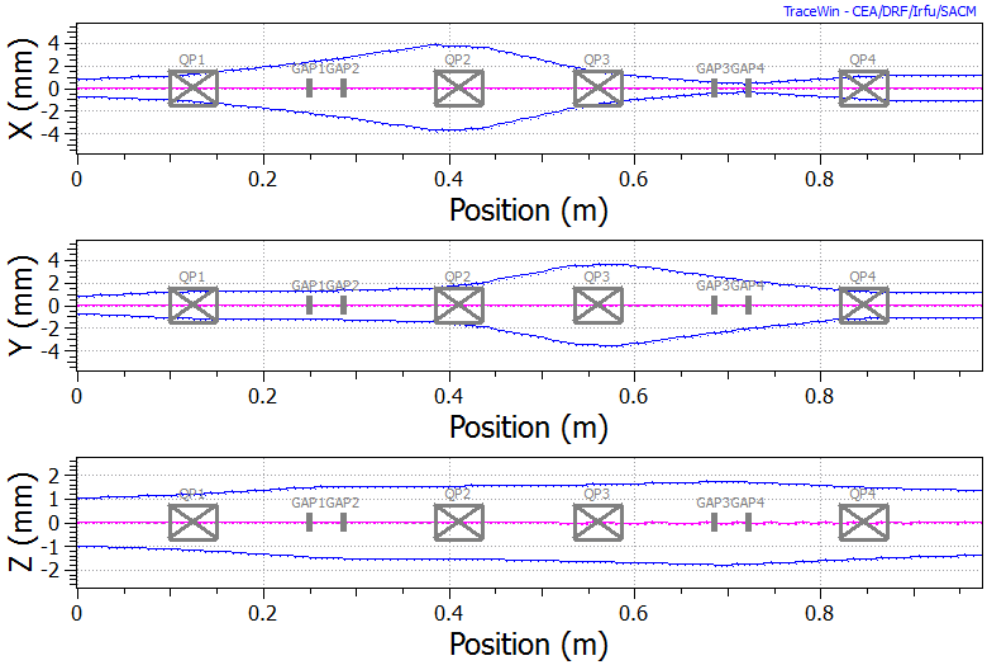

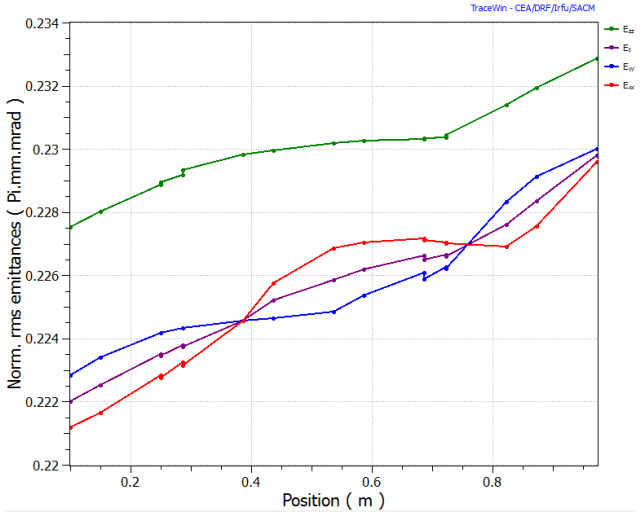

Emittance growth along MEBT

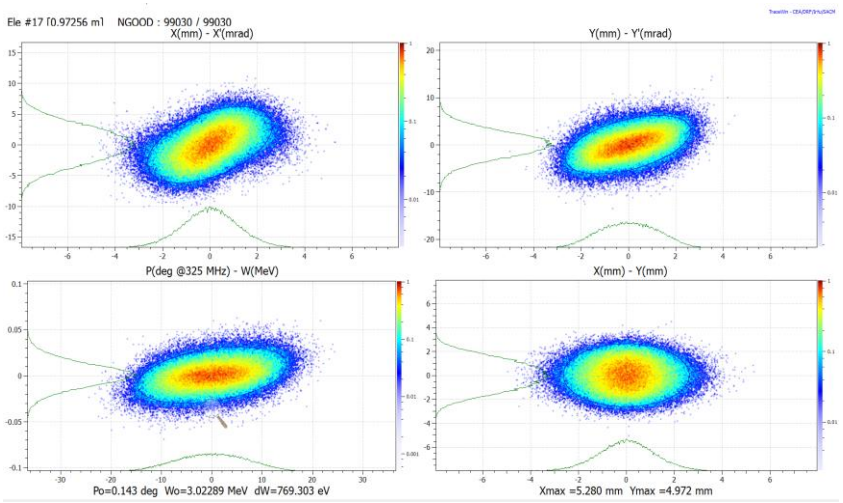

MEBT output beam distribution

SSR cavity design

- Three stages of spoke cavities named SSR-A with $\beta_g = 0.11$, SSR-B with $\beta_g = 0.22$ and SSR-C with $\beta_g = 0.46$ are chosen to accelerate a 3 MeV, 10 mA proton beam from RFQ to the final energy of 200 MeV.
- Electromagnetic and geometric parameters for each type of SSR are optimized to obtain maximum RF efficiency.
- Multipacting studies are also performed to check the secondary electron growth rate.
- R/Q for the higher order modes are calculated.

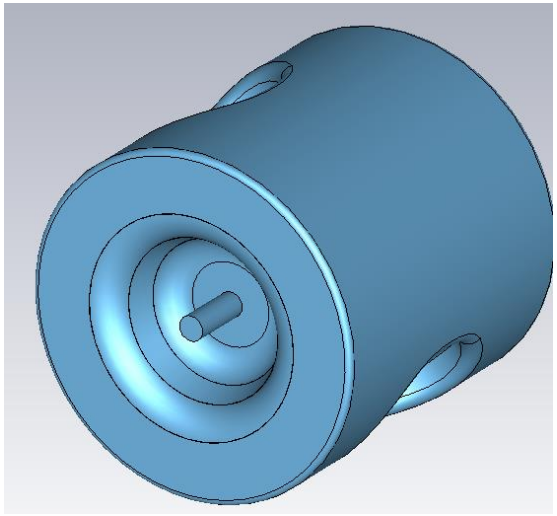

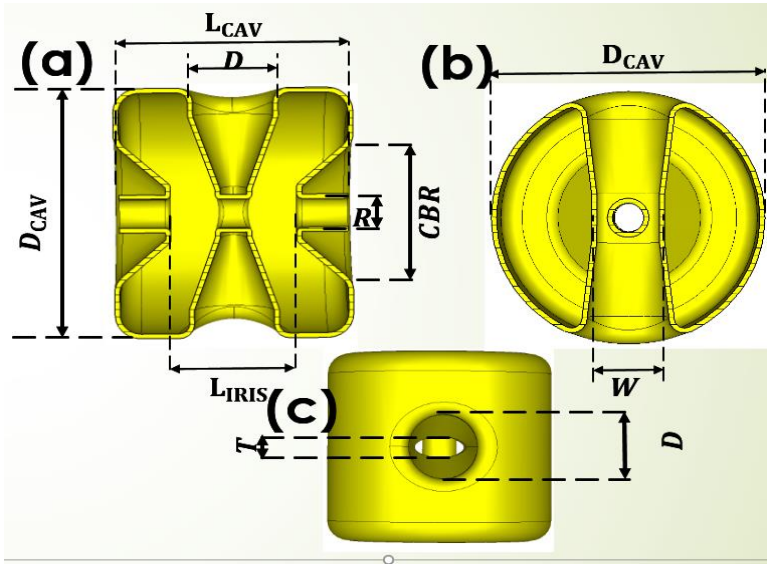

Electromagnetic design of single spoke resonators

Electromagnetic design of SSR cavity

Aim is to minimize Peak Surface fields

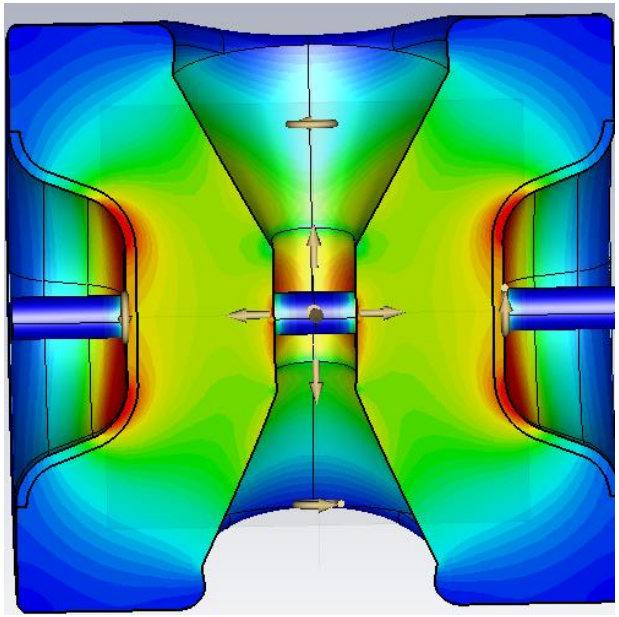

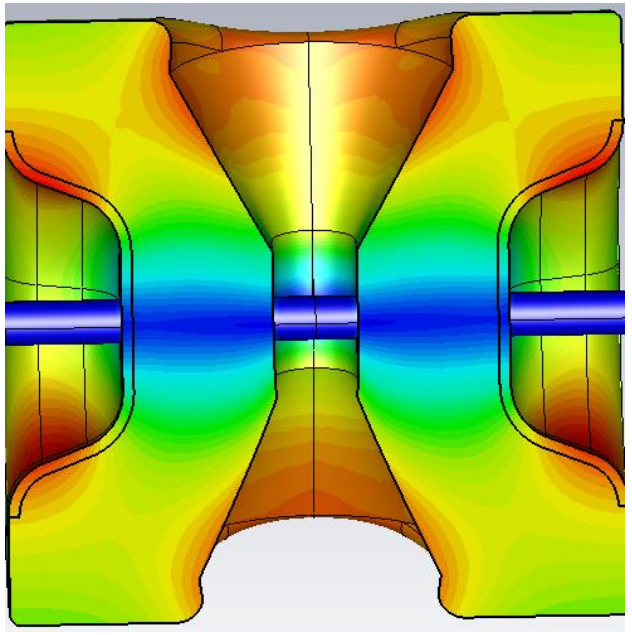

Electric field ***Magnetic field***

Minimize

E_P/E_0 *The ratio shows sensitivity of the shape to the field electron emission phenomenon.*

&

B_P/E_0 *The ratio shows limit in E_0 due to the break-down of superconductivity.*

Choice of optimal β

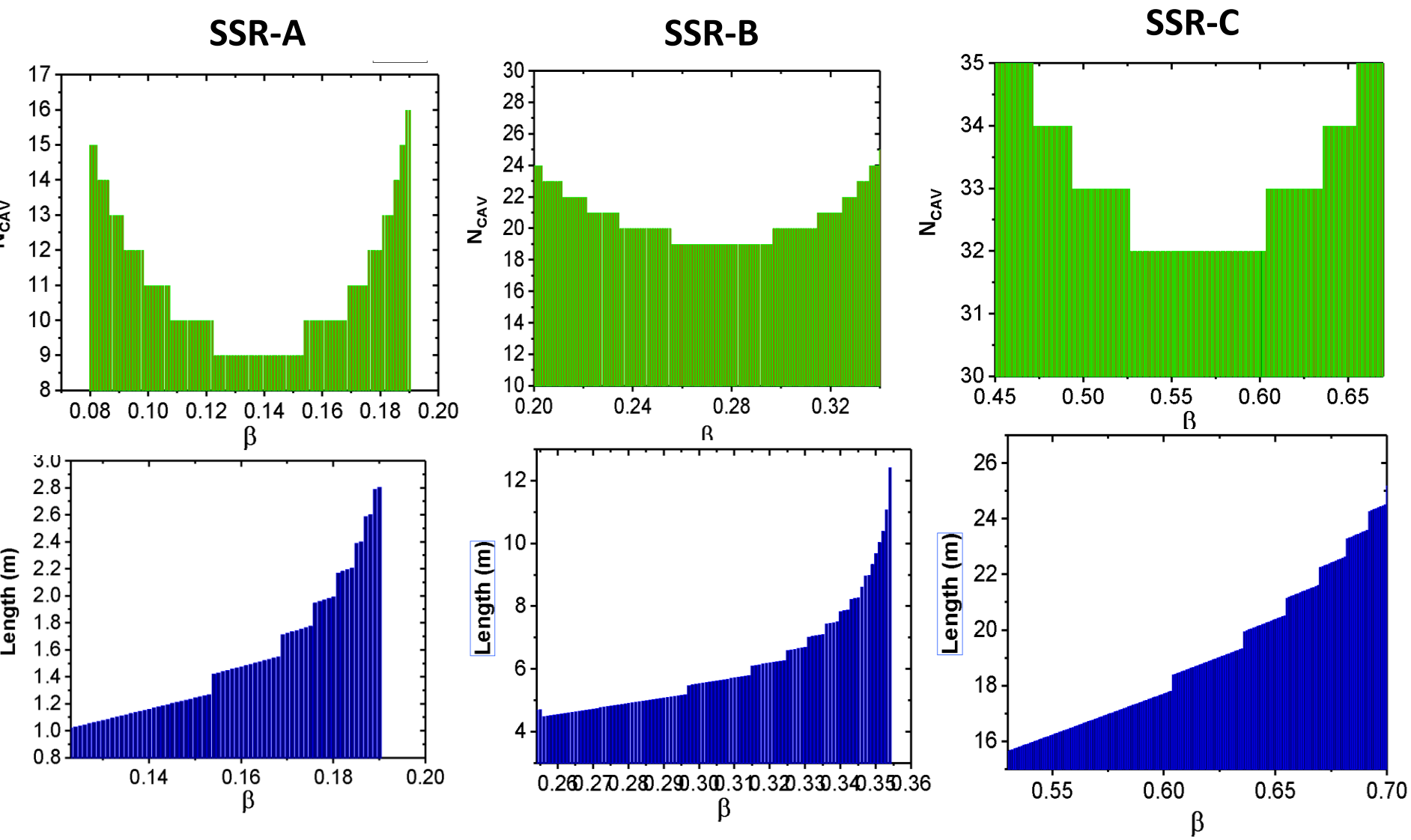

SSR-C: Design Optimization

Peak magnetic field optimization

Using an elliptical spoke base adds an extra parameter (D1 and D2) which can be used to optimize the peak magnetic fields.

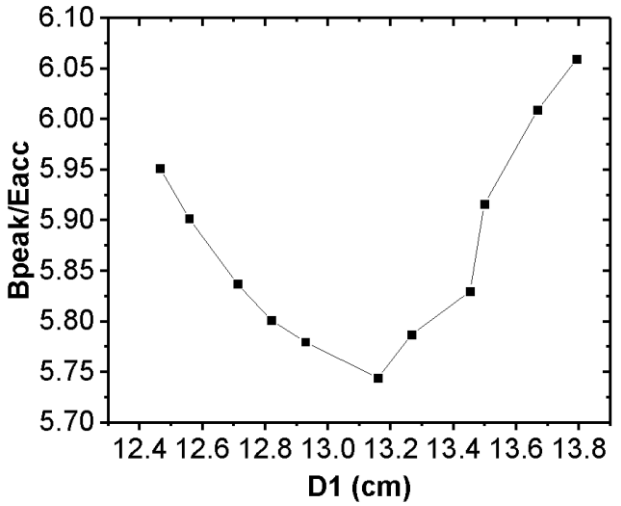

- **We observe a minimum value of 5.75 mT/(MV/m) for B_{PEAK}/E_{ACC}, at $D_1 = 13.1\ cm$.**

- **We observe a minimum value of 5.74 mT/(MV/m) for B_{PEAK}/E_{ACC}, at $D_2 = 13.15\ cm$.**

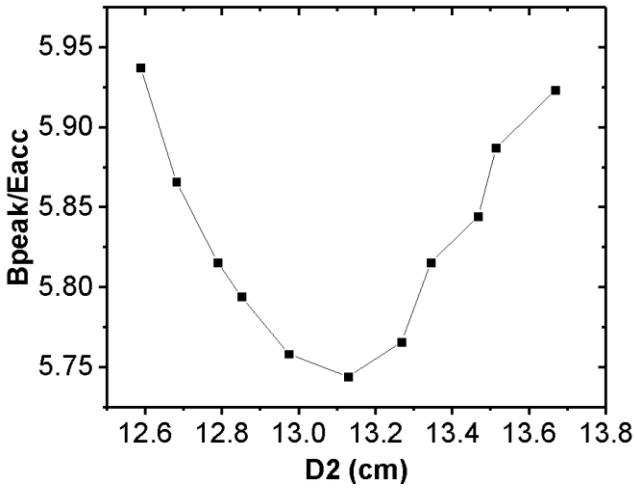

Variation in spoke base may change the E_{PEAK}/E_{ACC} values and hence the peak electric field with respect to T and W is optimized.

SSR-C: Design Optimization

Peak electric field optimization

- **We observe a minimum value of 3.46 for E_{PEAK}/E_{ACC}, at T= 3.81 cm.**
- **Variation of peak electric field with respect to the major axis of the spoke equator is observed to be small with a minimum value of 3.44 for E_{PEAK}/E_{ACC}, at W= 6.29 cm.**

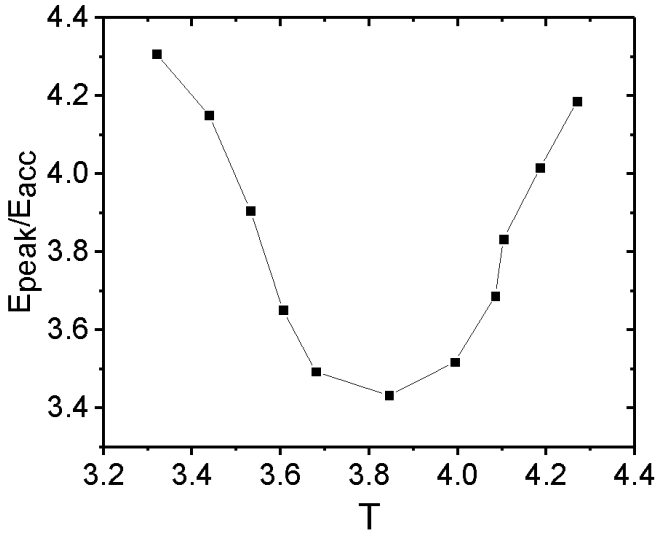

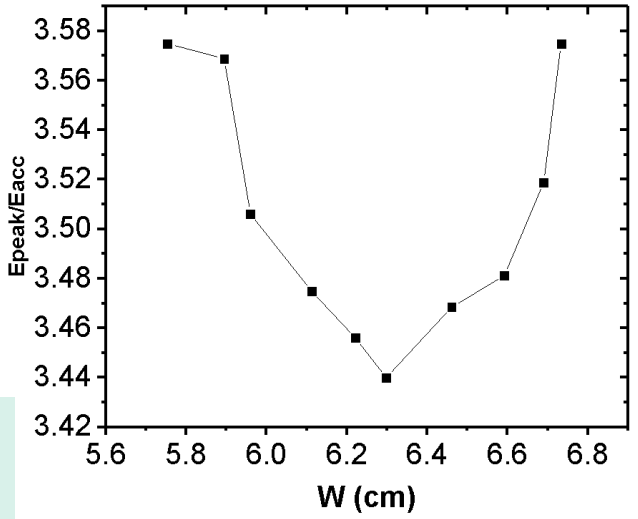

Final optimized parameters for a spoke with elliptical base

T= 3.81 cm
W=6.29 cm
D_1=13.1 cm
D_2=13.15 cm

E_{PEAK}/E_{ACC}	=	3.44
B_{PEAK}/E_{ACC}	=	5.74 mT/(MV/m)
R/Q	=	322 Ω

SSR: Design Optimization

SSR-A and SSR-B were also similarly optimized.

Parameter	SSR-A	SSR-B	SSR-C
Aperture radius (mm)	15	15	30
Effective Length (cm)	12.46	24.92	49.66
T (cm)	1.55	4.41	3.81
W	4.06	14.4	6.29
D1	6	7.6	13.1
D2	7	5	13.15
R/Q	128.8	223.6	322
E_{peak}/E_{acc}	4.75	3.49	3.44
B_{peak}/E_{acc} (mT/MV/m)	8.16	6.58	5.74
Accelerating Gradient (MV/m)	8	10	11

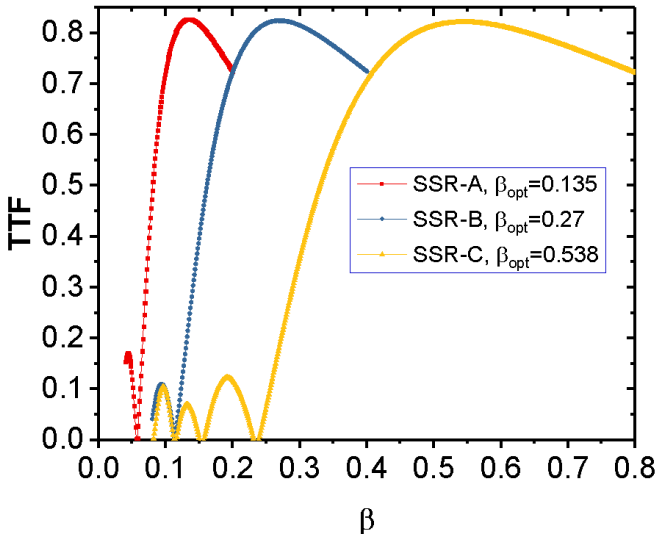

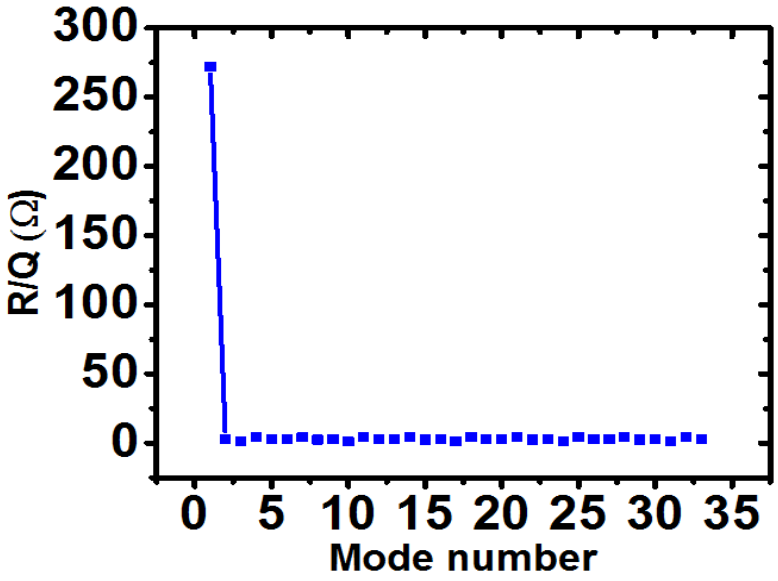

Multipacting Simulations

- Multipacting simulations were performed using MW CST, Particle-in–cell module.
- Systematic simulations were done to study the dependence of mesh density, particle number, number of bunches, initial electron energy and simulation time on the secondary electron emission yield. The results shows that, the growth rate is primarily determined by the mesh density and simulation time only.
- Multipacting studies were done on SSR-C cavities, using all surfaces, finite volume as well as ring electron sources and at different accelerating field gradients.

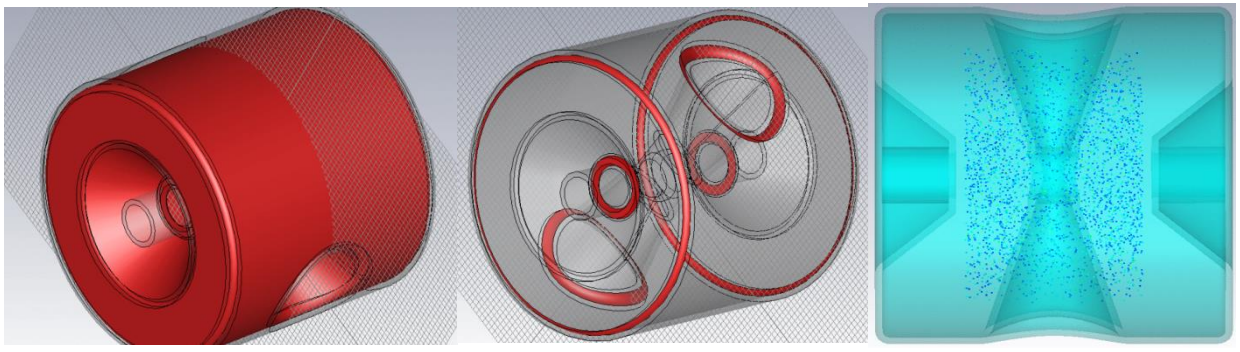

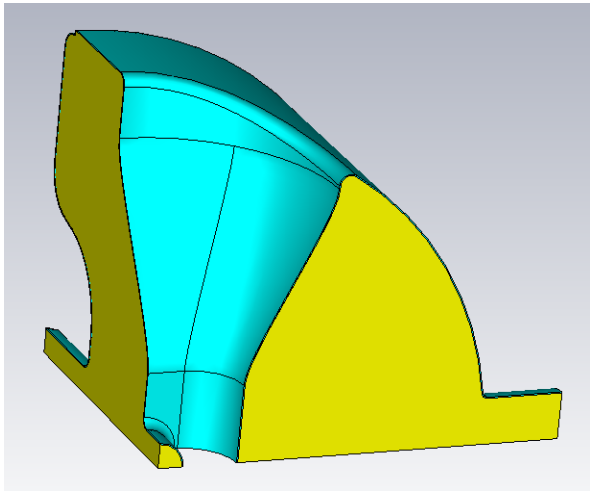

SSR-C: Multipacting Results

- SEY is calculated from emission and collision currents using the following expression,

$$SEY = \frac{I_{emission}}{I_{collision}}$$

- Obtained SEY was used to calculate the growth rate (α)

$$SEY = e^{\alpha T}$$

Where T is the RF Time period ($3\ ns$)

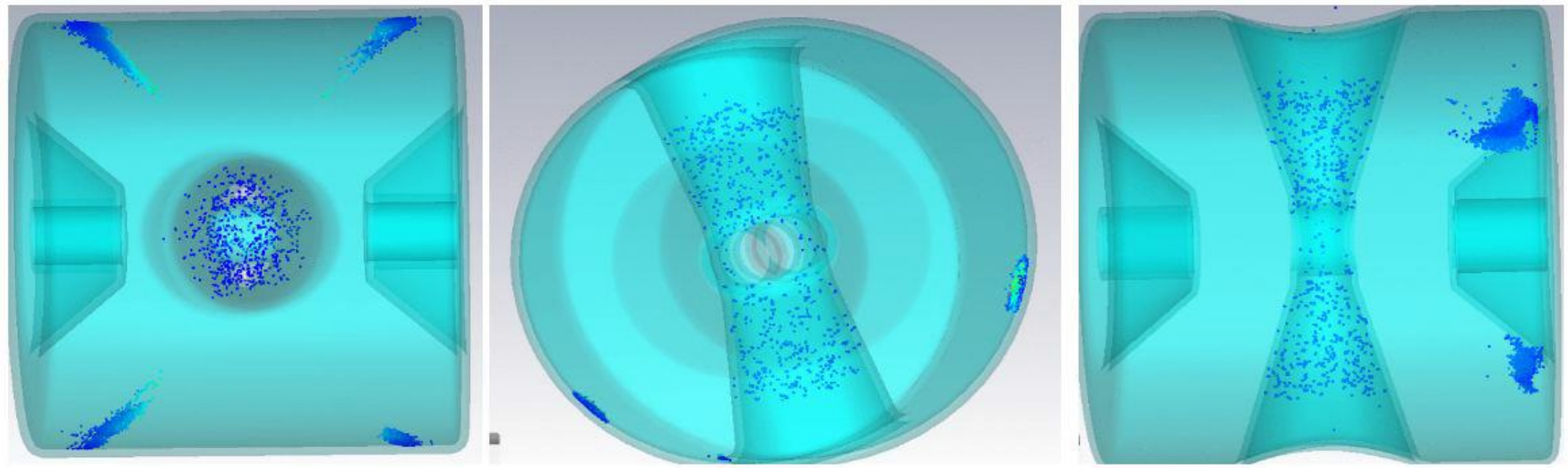

Electron density showing the multipacting sites in the SSR-C cavity.

SSR-C: Multipacting Results

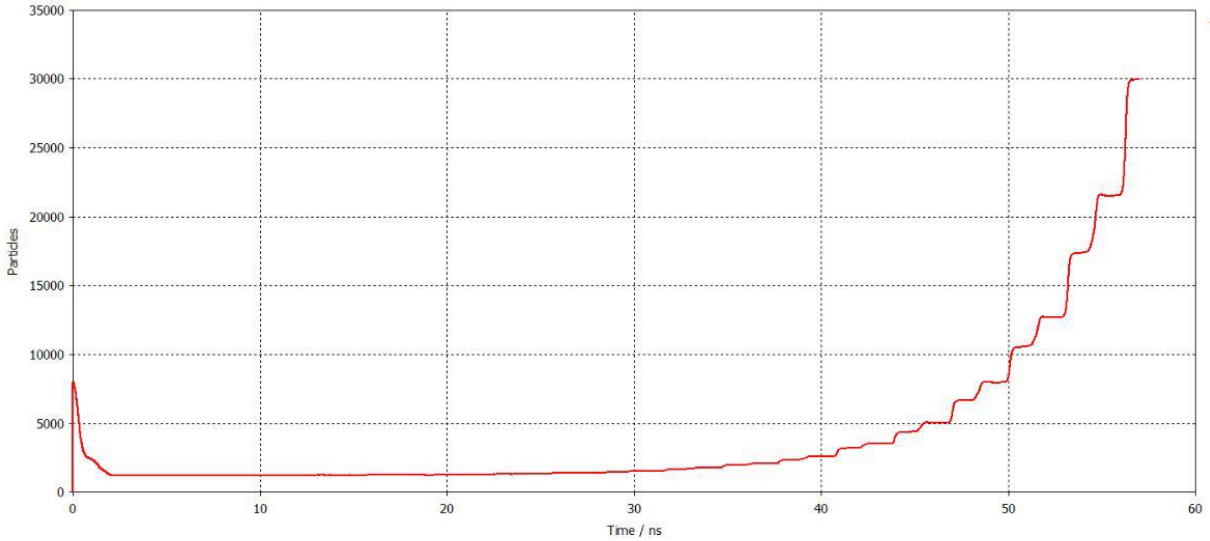

Cumulative particle number as a function of time showing multipacting in the SSR-C cavity.

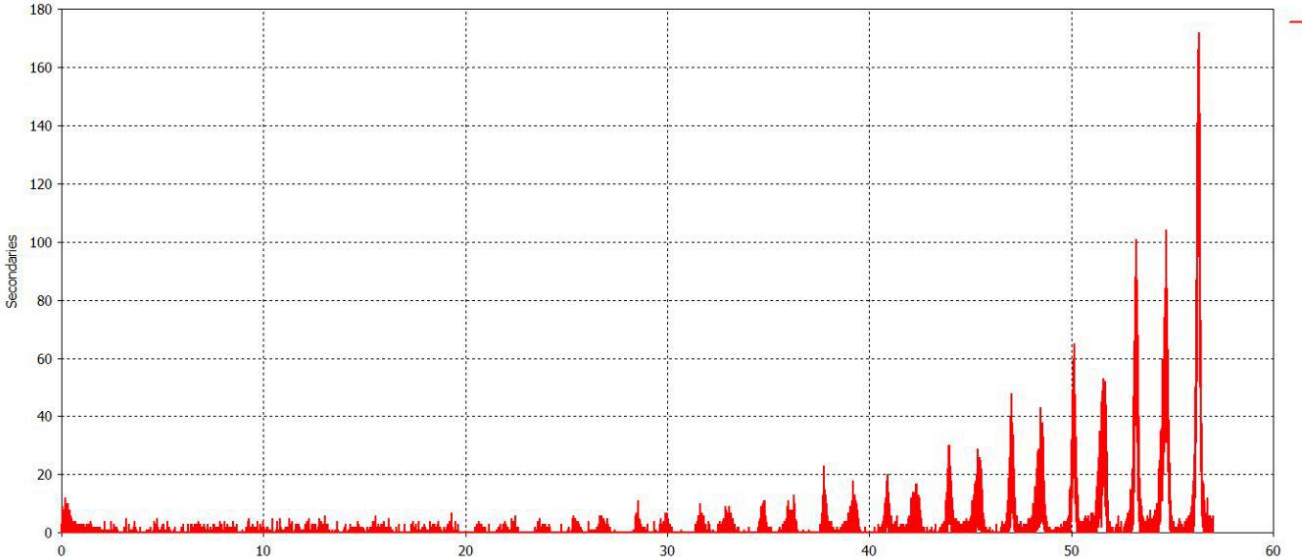

Instantaneous particle number with impact as a function of time within the SSR-C cavity.

SSR-C Corner curvature radius

In order to mitigate multipacting; it was found that double radius corners at the spoke end walls help in splitting the thick resonance barrier into thinner barriers thus making the multipacting process less severe. The radius of curvature need to be chosen carefully to avoid any kind of fabrication limits. So the effect different radii on multipacting as well as peak fields was studied.

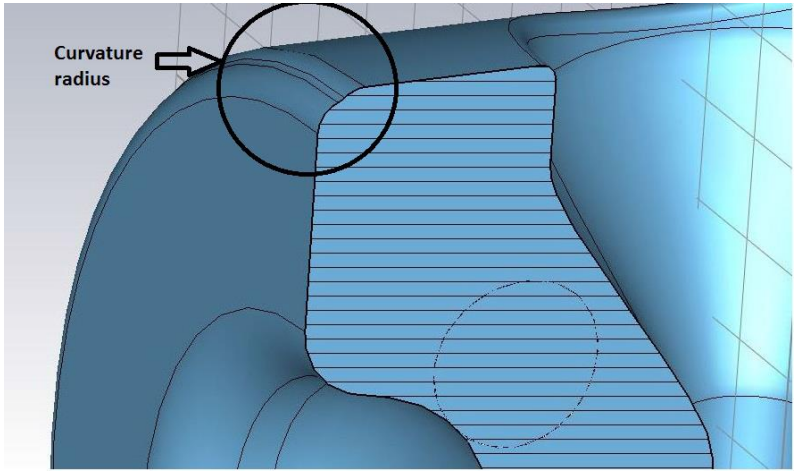

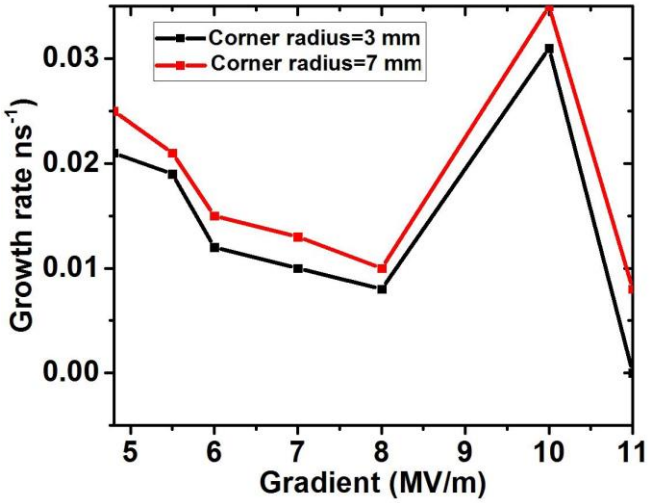

Radius (mm)	Gradient (MV/m)	E_{peak}/E_{acc}	B_{peak}/E_{acc} (mT/(MV/m))	R/Q (ohm)	Growth rate (nsec^{-1})
3	4.8	3.86	4.78	291	0.021
5	4.8	3.86	4.81	293	0.023
7	4.8	3.86	4.83	296	0.025
3	7	4.01	4.98	283	0.012
5	7	4.01	5.06	274	0.0135
7	7	4.01	5.18	270	0.014

Beam Dynamics in SSR

Main design issue:

☞ beam loss < 1 Watt/m.

☞ Low emittance increase.

☞ Minimize halo formation.

Design Philosophy

- Match the beam from one structure to the next.
- Smooth phase advance per metre across all transitions for current independent matching.
- Avoid instabilities by keeping the zero current phase advance per period in all planes below 90 deg.

SSR Linac design

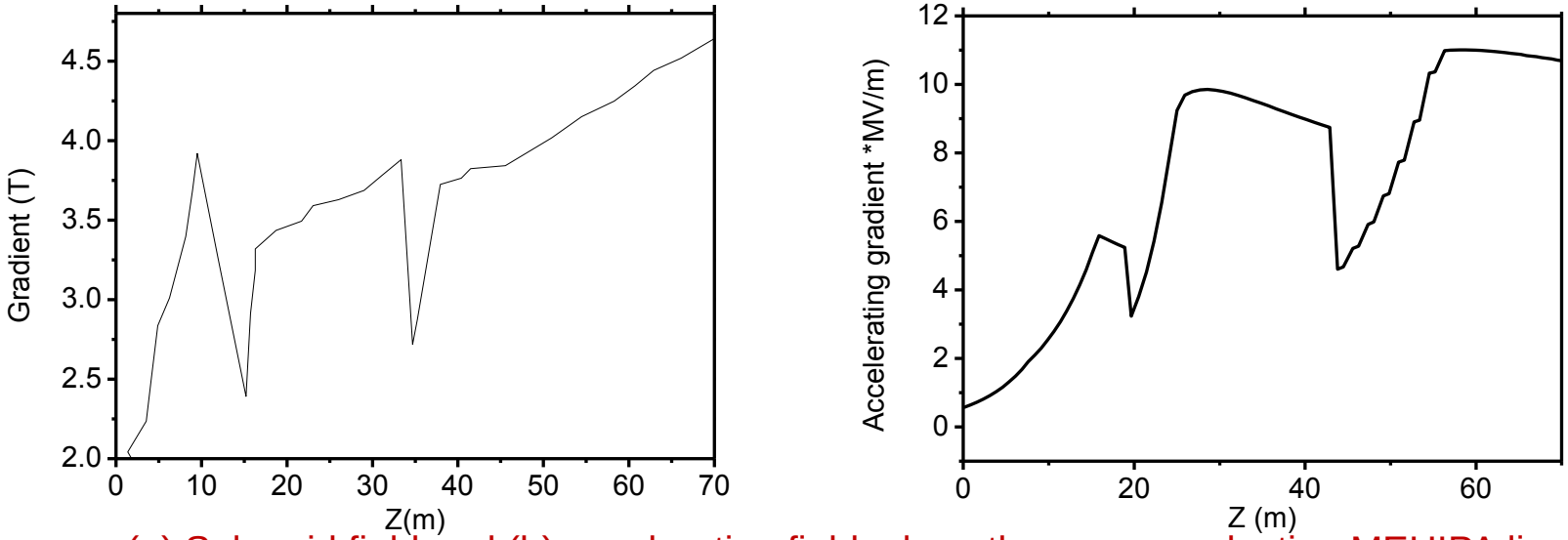

(a) Solenoid field and (b) accelerating field, along the superconducting MEHIPA linac.

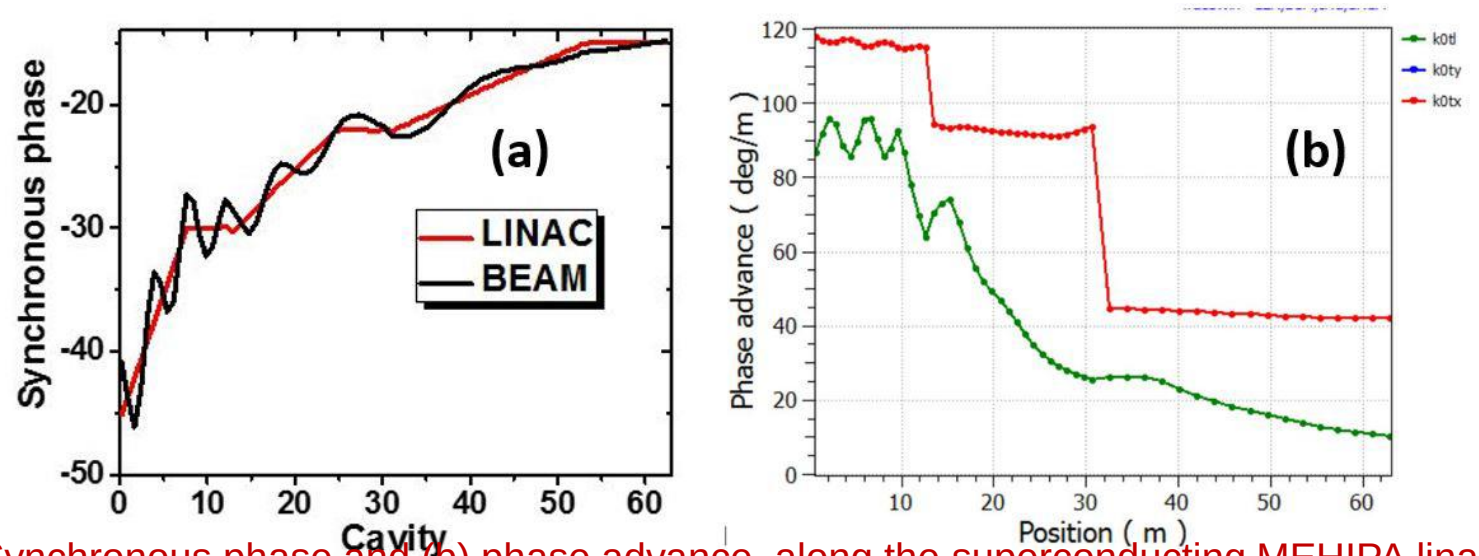

(a) Synchronous phase and (b) phase advance, along the superconducting MEHIPA linac.

SSR Linac design

SC linac lattice parameters

Parameter	SSRA	SSRB	SSRC
Energy range (MeV)	3 – 9.32	9.32-52.6	52.6-204
No. of solenoids	14	24	16
Eff. length of the solenoids	15 cm	30 cm	32 cm
Magnetic field of solenoids	2-3.8T	3.4-3.8 T	3.8.4.63 T
Synchronous phase	-45^{O} to -30^{O}	-30^{O} to -24^{o}	-24^{O} to -16^{o}
Length	9.12 m	22.89 m	39.34 m

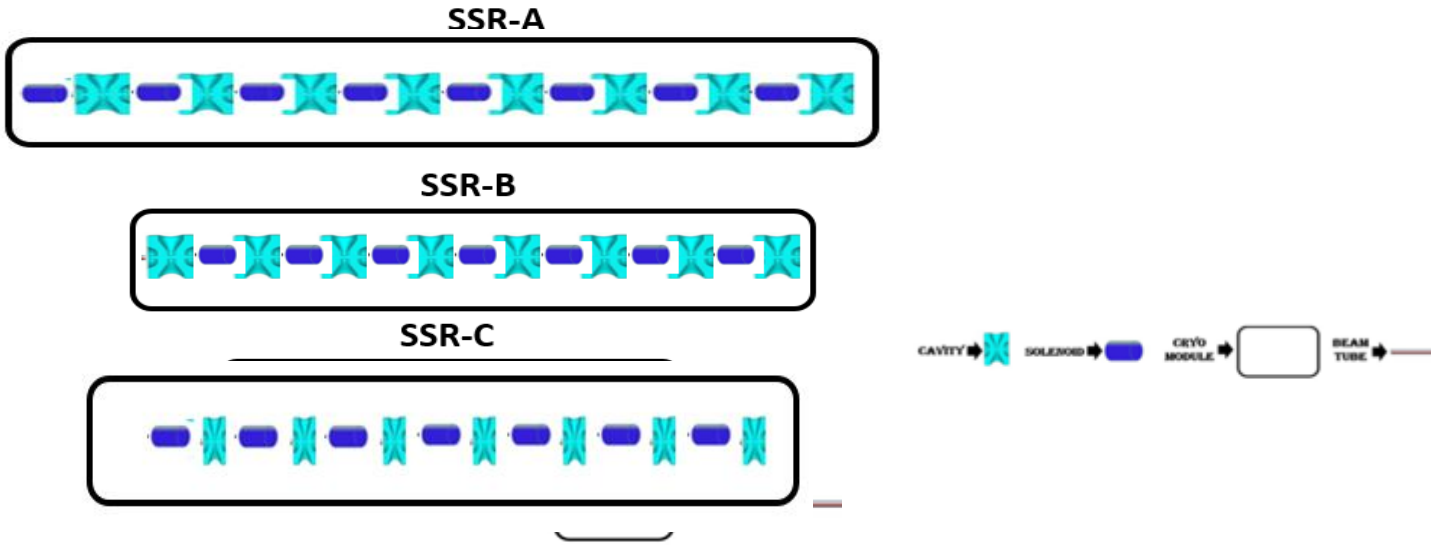

Cryomodule layout for the superconducting spoke resonators.

SSR beam dynamics

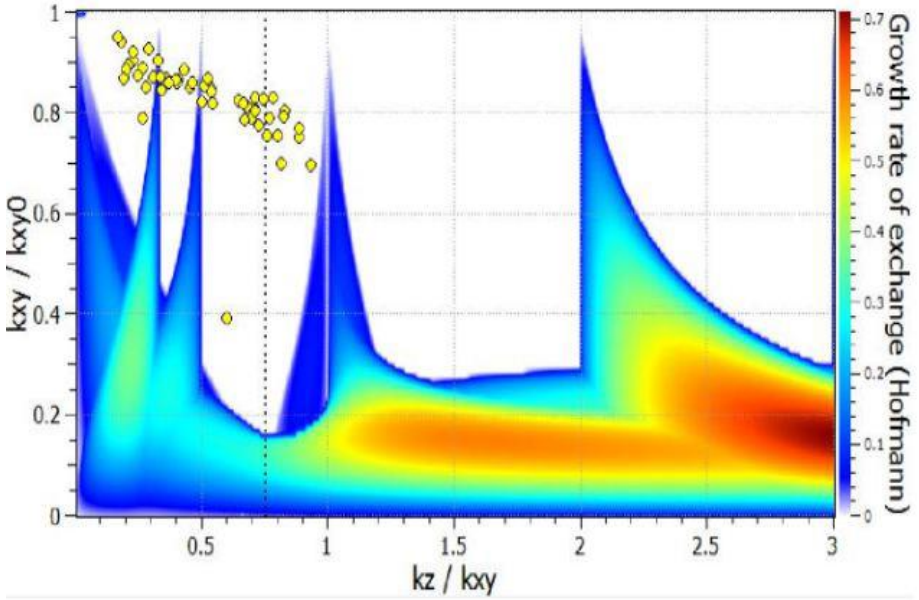

The instability at $k_z/k_t = 1$ has been completely avoided throughout so that there is no emittance exchange between the transverse and longitudinal planes.

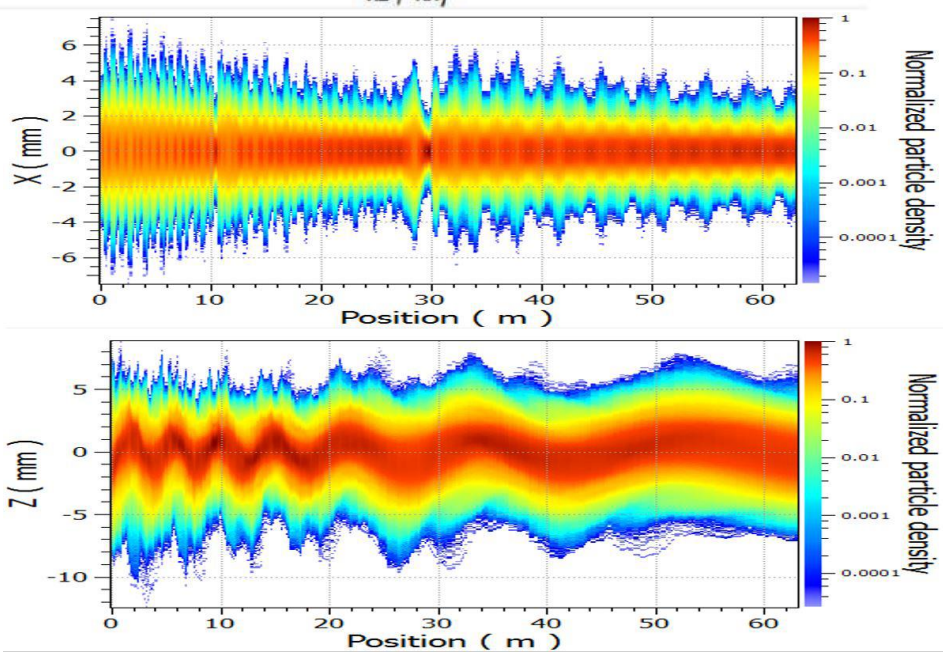

Beam profile through the linac

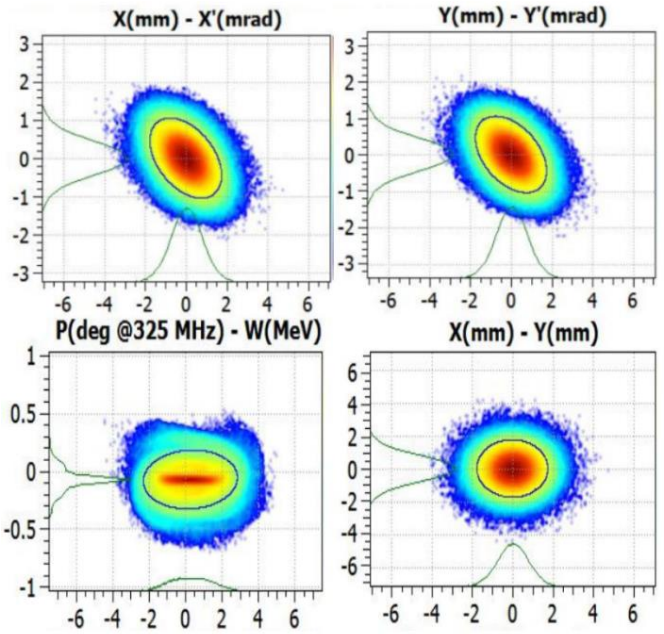

Beam at 200 MeV

SSR beam dynamics

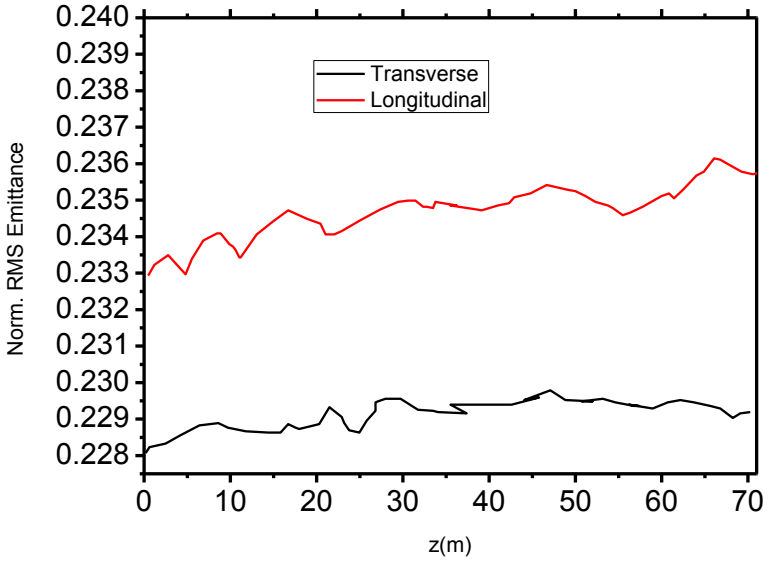

Beam Emittance

Output beam parameters of the MEHIPA linac

Parameter	SSR-A	SSR-B	SSR-C
ε_x (mm mrad)	0.229	0.229	0.229
ε_y(mm mrad)	0.23	0.23	0.23
ε_z(mm mrad)	0.234	0.235	0.23611
$Halo_x$	0.8	0.9	1.1
$Halo_y$	1.1	1	0.9
$Halo_z$	0.85	0.8	1
Transmission	100%	100%	100%

SSR RF Power Requirements

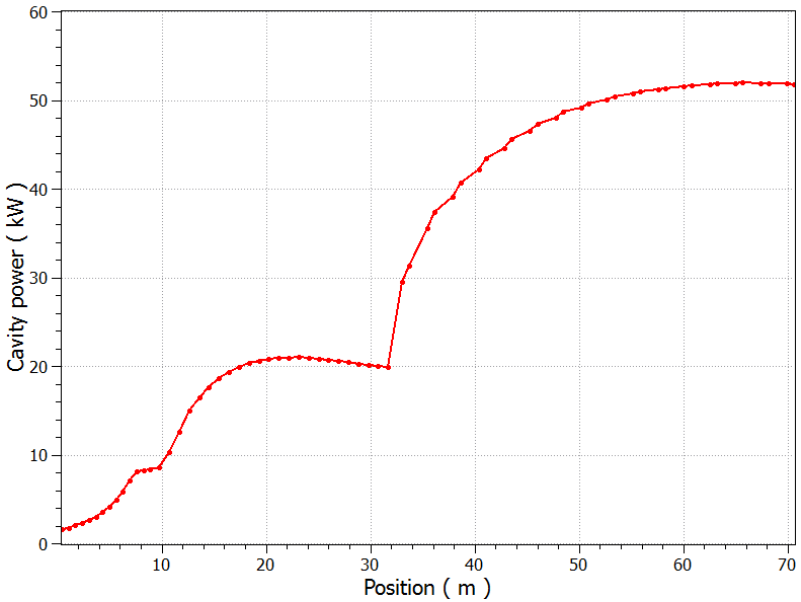

	F (MHz)	No. of RF cavities	No. of RF amplifiers per cavity	Beam Power	RF amplifier power (kW)
RFQ	325	1	1	3	400
SSRA	325	14	1	8	14.4
SSRB	325	24	1	21	61
SSRC	325	32	1	52	68.8

SSR: Cryogenic requirements

CM Type	Number of CMs	No. of cavities per CMs	Static load per CM (W)	Dynamic load per CM (W)	Total load at 2K per CM (W)	Total load at 2K
SSR-A	2	7	2.7	10	13.5	**27**
SSR-B	3	8	9.26	37	46.3	**139**
SSR-C	8	4	11.6	46.3	57.9	**463**
Total heat load = 629 W						